Separation Science and Technology
Publication details, including instructions for authors and subscription information:
http://www.informaworld.com/smpp/title~content=t713708471

Electrical Aspects of Adsorbing Colloid Flotation. XXII. Relaxation Times of Micellized and Adsorbed Surfactants

Matilal Sarker[a]; David J. Wilson[a]
[a] Department of Chemistry, Vanderbilt University, Nashville, Tennessee

To cite this Article Sarker, Matilal and Wilson, David J.(1988) 'Electrical Aspects of Adsorbing Colloid Flotation. XXII. Relaxation Times of Micellized and Adsorbed Surfactants', Separation Science and Technology, 23: 6, 661 — 686
To link to this Article: DOI: 10.1080/01496398808057658
URL: http://dx.doi.org/10.1080/01496398808057658

SEPARATION SCIENCE AND TECHNOLOGY, 23(6 & 7), pp. 661-686, 1988

Electrical Aspects of Adsorbing Colloid Flotation. XXII. Relaxation Times of Micellized and Adsorbed Surfactants

MATILAL SARKER and DAVID J. WILSON*

DEPARTMENT OF CHEMISTRY
VANDERBILT UNIVERSITY
NASHVILLE, TENNESSEE 37235

Abstract

Proton longitudinal relaxation times (T_1s) were measured for dodecyltrimethylammonium chloride (DTAC), dodecylammonium chloride, and sodium dodecylsulfate solutions in D_2O. Effects of added paramagnetic and diamagnetic salts on the various relaxation times were determined and interpreted in terms of the structures of the micelles. Relaxation times of DTAC adsorbed on $Al(OD)_3$–FeS floc were also determined and interpreted.

INTRODUCTION

Nuclear resonance techniques have been found to be of broad applicability in the study of surfactants (*1–3*). NMR methods have been used to monitor micelle formation (*4*, *5*); to study solubilization (*6*, *7*); to get information on micellar size, shape, and hydration (*8*); and to determine micellar aggregation numbers (*9*). NMR of counterions (such as sodium-23) has been used to determine the binding sites of the counterions on the micelles (*10*). The effects of electrolytes in surfactant solutions have been studied by several authors using NMR techniques (*11–15*). Tiddy et al. (*11*) studied the interactions between electrolytes and a zwitterionic surfactant using Na-23 and C-13 NMR. They found that positive adsorption of anions at the micelle surface occurs when salting-in electrolytes (such as NaSCN) are present, while negative adsorption of

---

*To whom correspondence should be addressed.

anions takes place with salting-out electrolytes (such as Na_2CO_3). Chobanau et al. (*12*) investigated the influence of pH and NH_4NO_3 concentration on the state of nonionic surfactants in solution. Zeev and Khalilov (*13*) studied the penetration of electrolytes into the hydroxyethyl layer of nonionic surfactants in the presence of metal salts. Kalibabchuk and D'yachek (*14*) observed that in the presence of alkali metal chlorides the exchange of free and aggregated sodium dodecylsulfate (SDS) ions decreases in the cation order $Li^+ < Na^+ < K^+ < Rb^+$, and that the corresponding order for anions is $SO_4^{2-} < Cl^- < I^-$. Kalyanasundaram et al. (*15*) used H-1 and C-13 NMR to study the electrolyte-induced phase transition from spherical to rod-shaped aggregates in aqueous micellar solutions of dodecylammonium chloride (DAC). The NMR lines of DAC become broader with increasing NaCL concentration. On the other hand, in dodecyltrimethylammonium chloride (DTAC) solutions, no line broadening was observed; the presence of the methyl groups in the micellar surface layer apparently prevents the electrolyte-induced aggregation of larger micelles.

In the present work we examine the proton spin-lattice relaxation times (T_1s) of DTAC, DAC, and SDS in micellar environments in the presence of various salts; measurements of DTAC adsorbed on ferrous sulfide–aluminum deuteroxide floc preparations are also discussed. It is known that micelle aggregation number increases with increasing added inert salt concentrations, while the size of spherical micelles remains essentially constant at a radius of roughly the length of the surfactant ion in an extended zigzag configuration (*16*, *17*). One therefore expects that the hydrocarbon chains of the surfactant ions will be more crowded and constrained in media of high ionic strength than in media of low ionic strength, and protons in different surfactant ions will be closer together; this should result in decreased proton T_1s. We present two theoretical models for the effect of ionic strength on aggregation number.

Earlier we investigated the adsorption of dodecylsulfate on $Al(OD)_3$ flocs by NMR techniques (*18*), and found that the orientation of the adsorbed surfactant could readily be determined by T_1 measurements. Insoluble sulfides are generally negatively charged, so should readily sorb cationic surfactants. In the present work we describe proton T_1 measurements which allow the determination of the orientation of DTAC ions adsorbed on FeS-$Al(OD)_3$ floc preparations.

REAGENTS AND EXPERIMENTAL PROCEDURES

Certified grade $MnSO_4 \cdot H_2O$, $Na_2S \cdot 9H_2O$, $FeSO_4 \cdot 7H_2O$, $K_3(FeCN)_6$, NaCl, Na_2SO_4, Na_2S and $FeSO_4$ were purchased from Fisher. Anhydrous

$MnSO_4$, Na_2S, and $FeSO_4$ were prepared by heating the hydrated compounds *in vacuo* for 10–18 h. Aluminum metal was obtained from Welch. MSD Isotopes supplied D_2O, NaOD, D_2SO_4, and DCl. SDS of 99+% purity was obtained from Sigma; its cmc was determined in an earlier study (*19*) and found to be in good agreement with previously published values. DTAC was obtained from Eastman; determination of its cmc by conductivity titration gave a value of 1.85×10^{-2} *M*; Mukerjee and Mysels reported a value of 2.03×10^{-2} *M* (*20*). Dodecylamine was obtained from Aldrich; its cmc at pH 2.3 was 1.35×10^{-2} *M*, and at 7.0 it was 1.0×10^{-2} *M*. Mukerjee and Mysels (*20*) report a value of 1.46×10^{-2} *M* for the cmc of the ionic form. The DAC stock solution for the NMR experiments was made by reacting 0.9561 g dodecylamine with 0.5494 g of 35% w/w DCl solution and adjusting the volume to give a DAC concentration of 0.5028 *M*. The pD of this solution was 6.8.

The NMR experiments were carried out on a JEOL FX-90Q Fourier transform spectrometer operating at 89.55 MHz. The inversion-recovery method (a 180°-*t*-90°-FID sequence) was used to measure the T_1*s*. The values of *t* and the number of accumulations were selected depending on the sample characteristics. The data thus obtained (sets of values of t, $M_z'(t)$, and *NG*) were then used to get a nonlinear least squares fit to the equation

$$M_z(t) = M_0[1 - 2\exp(-t/T_1)] \tag{1}$$

where $M_z = M_z' \times 2^{NG}$
NG = instrument normalized gain of M_z
M_0 = equilibrium magnetization
T_1 = spin-lattice relaxation time
t = interval between the 180° and 90° pulses

Standard 5 mm NMR tubes were used, and nonsurfactant solutions were purged with nitrogen. Surfactant solutions were made up with nitrogen-purged D_2O and kept under nitrogen; after the NMR samples were made up, the tops of the tubes were flushed with nitrogen.

It was found that the duration of a 180° pulse varied somewhat from sample to sample, depending on the salt concentration. Therefore the duration of a 180° pulse was measured frequently. Measurements of peak height as a function of pulse duration in a one-pulse experiment yield a sine curve; the first null point of this (after $t_p = 0$) gives the duration of a 180° pulse. In all cases 3-(trimethylsilyl)-propanesulfonic acid, sodium salt (DSS) was used as an internal reference.

Stock solutions of the surfactants were made up by weight in D_2O as follows. A 1.0369 g portion of DTAC was dissolved in D_2O and diluted to

20.00 mL to give a 0.1965 *M* solution. 0.7161 g SDS was dissolved in D_2O and diluted to 10.00 mL to make up a 0.2056 *M* solution. Stock solutions of salts were made up in D_2O as follows. Anhydrous solid salts were weighed out, dissolved in D_2O, and diluted volumetrically to make 1.0083 *M* Na_2SO_4, 5.0072 *M* NaCl, 0.9974 *M* $MnSO_4$, and 0.9974 *M* $K_3Fe(CN)_6$. Samples containing concentrations of Na_2SO_4 1 *M* and above were prepared by weighing out the required amount of anhydrous Na_2SO_4, adding DTAC stock solution, and diluting to the appropriate volume.

It was found that precipitates consisting of metal sulfides alone were rapidly coagulated and settled on the addition of surfactants, making it impossible to use these in NMR experiments. Therefore a mixed floc consisting of FeS and $Al(OD)_3$ was prepared in the hope that it would have the settling characteristics of $Al(OD)_3$, which we had previously found could be used for NMR studies of adsorbed surfactants, would have the extremely large specific surface of $Al(OH)_3$, and would carry the negative surface charge commonly associated with sulfide precipitates. This mixed floc was prepared as follows. $Al_2(SO_4)_3$ was prepared by reacting 0.2262 g aluminum metal with 1.2850 g D_2SO_4 and filtering the resulting solution. 2.00 mL of this solution was then added to 2.00 mL of 0.1093 *M* $FeSO_4$ in D_2O. The pD was then adjusted to 11.5, and 1.5 mL of 0.2737 *M* Na_2S in D_2O was added. This gave a mixed precipitate of $Al(OD)_3$ and FeS; this was then washed four times with D_2O to remove SO_4^{2-} and Na^+, then it was suspended in D_2O. The final volume of the suspension was 12 mL, and its pD was 5.6. Nitrogen was then passed through the suspension to remove dissolved oxygen, and this stock suspension was stored under nitrogen. From the quantities of the starting materials, the solid phase should have contained about 20% FeS and 80% $Al(OD)_3$ by weight. The sedimentation rate of this suspension was slow enough so that NMR experiments could be carried out conveniently. For the NMR runs, 0.5 mL of this suspension was placed in an NMR tube and the desired amount of surfactant solution was added; the total quantity of FeS was constant in all the DTAC–FeS experiments.

EXPERIMENTAL RESULTS

Spectra of DTAC at concentrations below (9.82×10^{-3} *M*) and far in excess (0.1022 *M*) of the cmc are shown in Figs. 1 and 2. The peak assignments were made by comparison with the reference spectrum for dodecyltrimethylamonium bromide (*21*). The peak centered at $\delta = 0.8391$ ppm is assigned to the terminal methyl protons; that centered at 1.2562 ppm to the bulk of the methylene protons; that at 3.0866 to the *N*-methyl

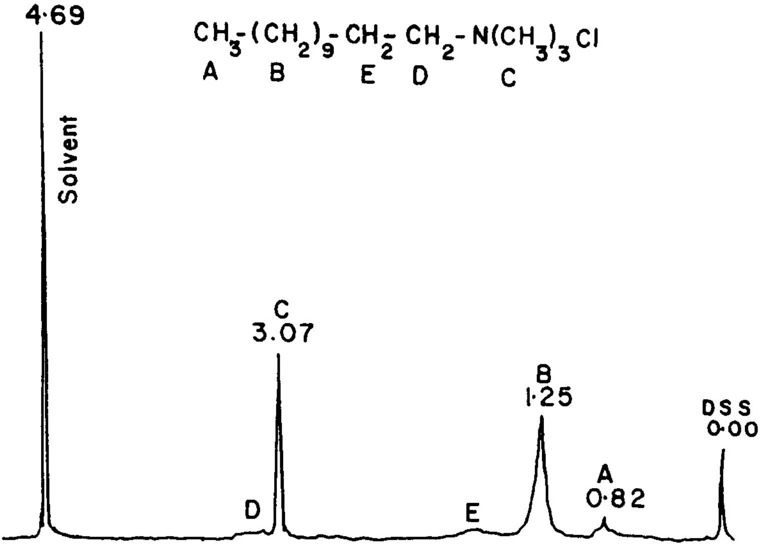

FIG. 1. Proton NMR spectrum of 9.82 m*M* DTAC in D_2O. Spectrometer frequency 89.55 MHz, 32 accumulations, pulse length 20 μs, acquisition time 2.273 s, reference DSS.

protons. The small peak downfield from the *N*-methyl peak is due to the α-methylene group, and the hump immediately downfield from the large methylene peak at 1.2562 ppm is due to the β-methylene protons. The peak at $\delta = 4.6667$ ppm is due to the HDO protons. The chemical shifts change slightly as one goes from lower to higher concentrations, but the changes in chemical shifts are sufficiently small to be of relatively little help in studying micelle formation. We therefore turned to T_1 measurements on the terminal methyl, the bulk methylene, and the *N*-methyl protons.

The results of T_1 measurements on DTAC solutions are shown in Fig. 3, in which the relaxation rates ($1/T_1$) are plotted against DTAC concentration. The relaxation rates are apparently linear functions of the concentration over the range studied, with the rates of increase of relaxation rate in the order bulk methylene > *N*-methyl > terminal methyl.

The effects of added salts of various types on surfactant proton relaxation times were then investigated. A cationic surfactant (DTAC) and an anionic surfactant (SDS) were studied; the concentrations of both surfactants were held constant at 0.102 *M*, far above their cmc's.

In Fig. 4 we see the relaxation rates of DTAC protons plotted against

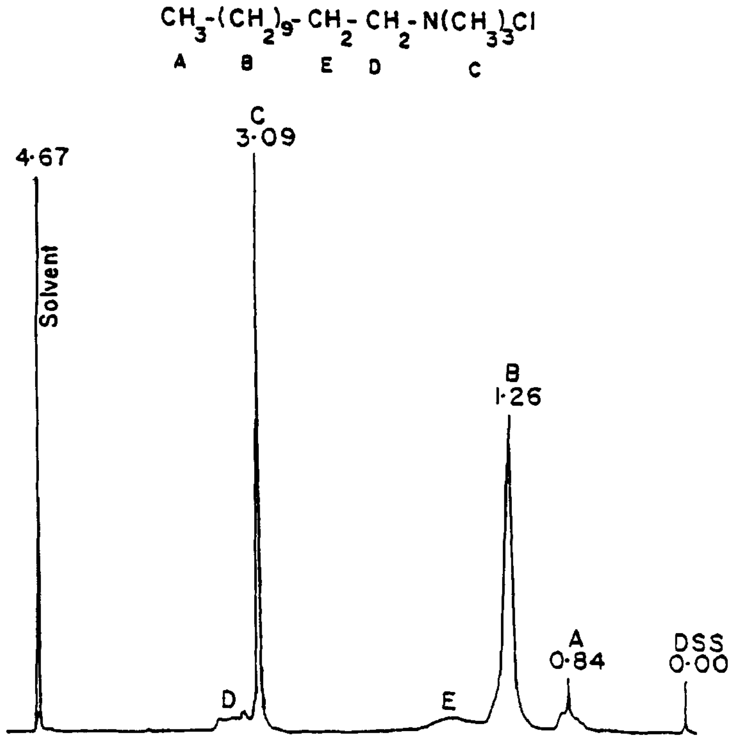

FIG. 2. Proton NMR spectrum of 0.1022 *M* DTAC in D_2O. Conditions as in Fig. 1.

the concentration of added Mn^{2+}. Manganous ion is paramagnetic, so should markedly increase the relaxation rates of those protons which can be closely approached by the ion. This effect should be somewhat reduced by the fact that coulombic repulsions will tend to keep the positive DTAC micelles and the positive Mn^{2+} ion apart. It is evident from the slopes of the plots that the rate of change in relaxation rate is largest for the *N*-methyl protons, presumably due to the ionic-$N(CH_3)^+$ groups being on the surface of the micelle so that the manganous ions can approach these protons more closely than any of the others.

These effects are due to the Mn^{2+} ions, not sulfate, as indicated by comparing the data from Fig. 4 with the data shown in Fig. 5, which gives results for experiments in which the concentration of SO_4^{2-} was kept constant by addition of the appropriate quantities of Na_2SO_4 as the concentration of $MnSO_4$ was varied. The slopes of the relaxation rate plots of the terminal methyl and bulk methylene protons are virtually

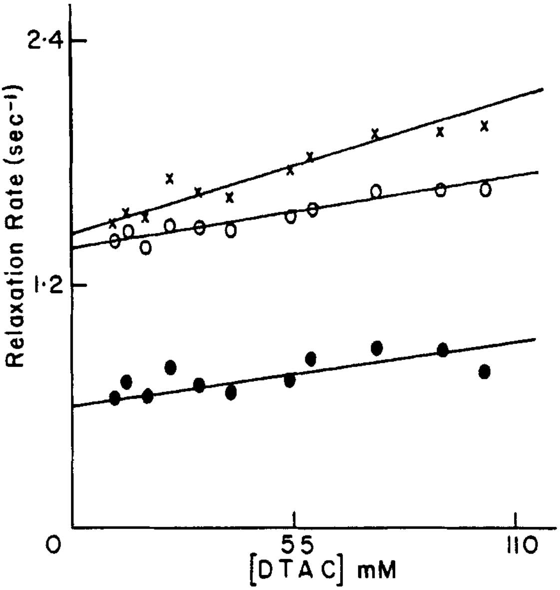

FIG. 3. DTAC proton relaxation rates ($1/T_1$) versus DTAC concentration (m*M*). Slopes from top to bottom: bulk methylene, 4.92 ± 0.94; *N*-methyl, 2.85 ± 0.61; terminal methyl, 1.83 ± 0.64 s^{-1} M^{-1}.

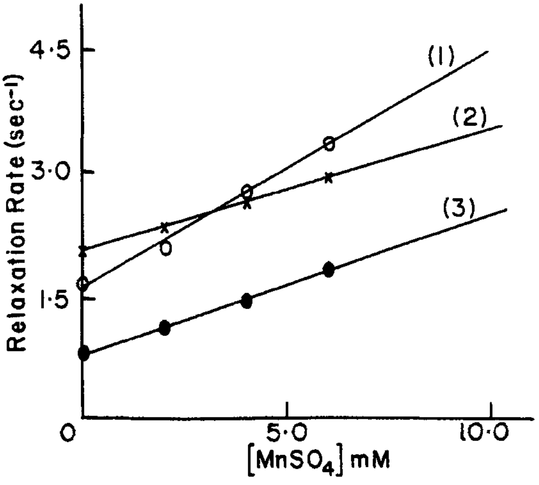

FIG. 4. DTAC proton relaxation rates versus Mn^{2+} concentration. [DTAC] = 0.1022 *M*. Slopes are as follows: (1) *N*-methyl, 290; (2) bulk methylene, 163; (3) terminal methyl, 174 s^{-1} M^{-1}.

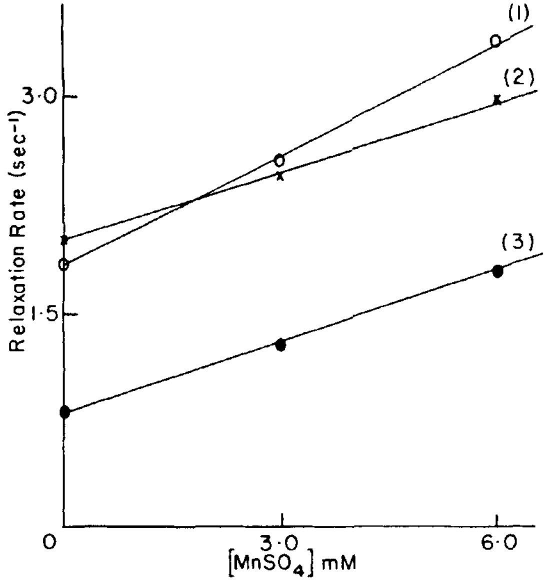

FIG. 5. DTAC proton relaxation rates versus Mn^{2+} at constant [SO$_4^{2-}$] = 6.0 m*M*, [DTAC] = 0.1022 *M*. Slopes are (1) *N*-methyl, 258; (2) bulk methylene, 162; terminal methyl, 169 s^{-1} *M*$^{-1}$.

identical in the two sets of plots; the *N*-methyl relaxation rates show what might be a slight effect of sulfate.

The results of relaxation time measurements on SDS solutions with varying concentrations of Mn^{2+} are shown in Fig. 6. The effects are enormously greater than found with DTAC; this is to be expected with an anionic surfactant, since the coulombic forces now are attracting Mn^{2+} ions into the vicinity of the negatively charged micelles. As expected, the protons nearest to the surface of the micelles (the α-methylene protons) are most affected.

Figures 7 and 8 show the effects of the paramagnetic anion Fe(CN)$_6^{3-}$ on the relaxation rates of DTAC and SDS protons. The effects are somewhat less than those observed with Mn^{2+}, but increases in relaxation rates are observed, particularly for the *N*-methyls in DTAC, as expected. Initially K$_3$Fe(CN)$_6$ reacted with DTAC to form a yellow solid; this dissolved on vigorous shaking, but it is possible that compound formation is complicating these results.

We next turn to the effects of diamagnetic salts on the proton relaxation times of DTAC in micelles. Figure 9 displays plots of

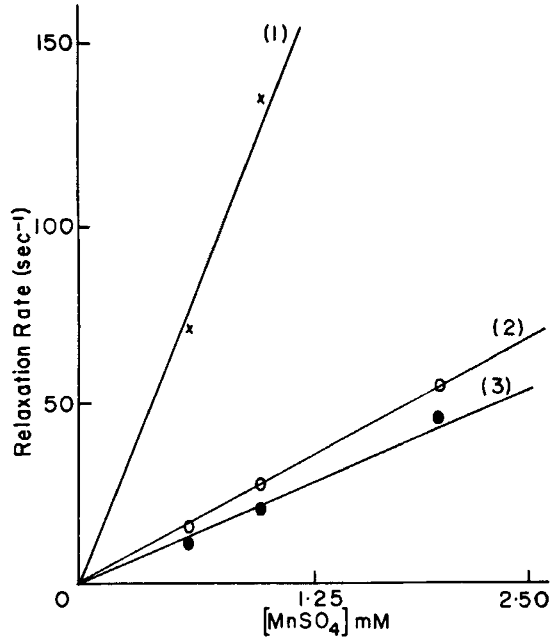

FIG. 6. SDS proton relaxation rates versus [Mn^{2+}]. [SDS] = 0.1088 *M*. Slopes are (1) α-methylene, 1.33×10^5; (2) bulk methylene, 2.69×10^4; (3) terminal methyl, 2.30×10^4 s^{-1} M^{-1}.

relaxation rates versus sodium sulfate concentration. (Note that the abscissa here has units of mol/L, while the abscissas of plots involving paramagnetic salts have units of mmol/L.) All the relaxation rates measured increase with increasing Na_2SO_4 concentration, indicating that all of the protons are more constrained in their motions. Figure 10 exhibits plots of relaxation rates against sodium chloride concentration; here also the relaxation rates increase with increasing salt concentration, although the effects are less than those observed with Na_2SO_4. These results indicate that the surfactant ions are more crowded in solutions of higher ionic strength. This is consistent with the comments of Vold and Vold (*16*) that spherical micellar radii remain approximately equal to the extended length of surfactant ion, but that the aggregation numbers of surfactant micelles increase with increasing salt concentration. We shall address the theoretical aspects of this later in this paper.

We next turn to measurements of DTAC proton relaxation times in the presence of $Al(OD)_3$ and $FeS-Al(OD)_3$ flocs. As mentioned earlier, it was

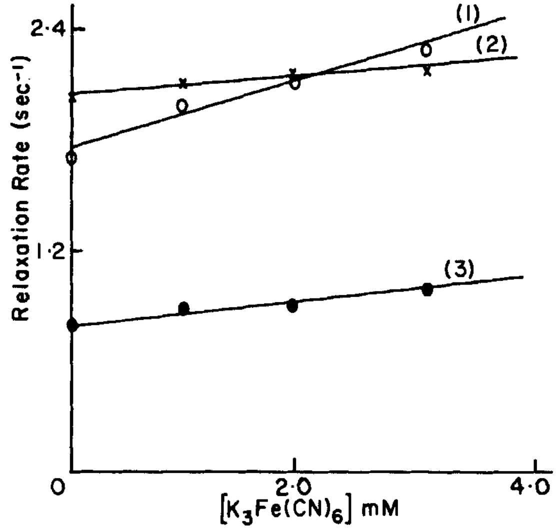

FIG. 7. DTAC proton relaxation rates versus [Fe(CN)6^{3-}]. [DTAC] = 0.1022 *M*. Slopes are (1) *N*-methyl, 177; (2) bulk methylene, 48; (3) terminal methyl, 59 s^{-1} M^{-1}.

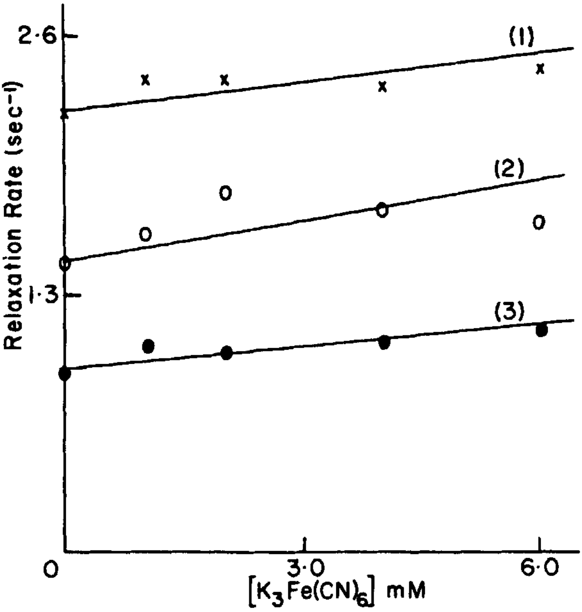

FIG. 8. SDS proton relaxation rates versus [Fe(CN)$_6^{3-}$]. [SDS] = 0.1088 *M*. Slopes are (1) bulk methylene, 52.9; (2) α-methylene, 4.64; (3) terminal methyl, 42.6 s^{-1} M^{-1}.

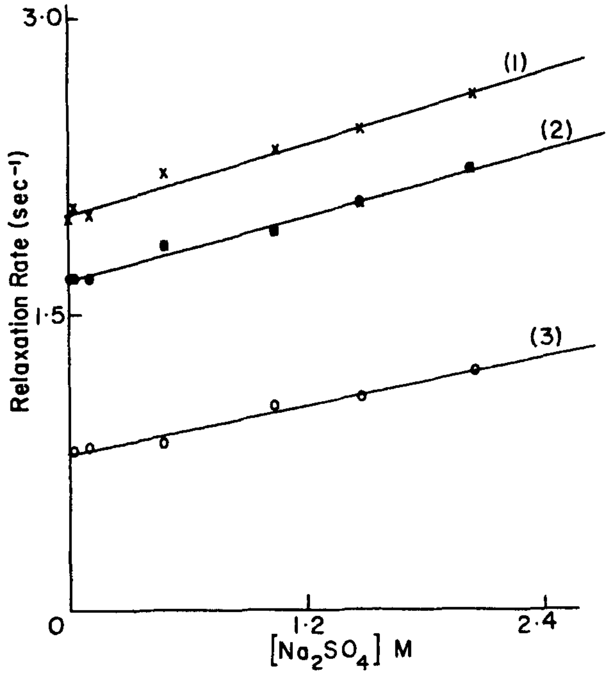

FIG. 9. Effect of [Na_2SO_4] on DTAC proton relaxation rates. [DTAC] = 0.1022 *M*. Slopes are (1) bulk methylene, 0.277; (2) *N*-methyl, 0.220; (3) terminal methyl, 0.205 s^{-1} M^{-1}.

not possible to prepare FeS precipitates which would remain in suspension long enough in the presence of DTAC to permit NMR measurements. Figures 11 and 12 present NMR spectra of 0.0136 *M* and 0.1046 *M* DTAC in the presence of the FeS–$Al(OD)_3$ floc. A comparison of Fig. 11 with Fig. 1 shows that the peaks in Fig. 11 are much broader than those in Fig. 1, and that the signal-to-noise ratio is substantially lower. At this relatively low concentration of DTAC, probably most of the DTAC ions are adsorbed on the solid FeS, so the proton relaxation rates are high because of both physical constraints and paramagnetic relaxation. A comparison of Fig. 2 with Fig. 12 shows that the peaks are broader in Fig. 12, but the contrast is not nearly as great as it is at the lower concentration. Presumably at the higher surfactant concentration the limited amount of FeS present can adsorb only a fraction of the DTAC, leaving substantial amounts in solution either as free ions or in micelles.

Relaxation rates of DTAC protons in the presence of FeS–$Al(OD)_3$ at

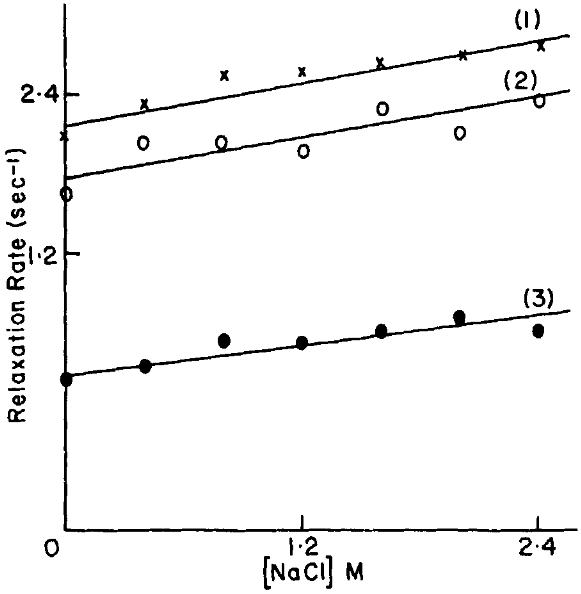

FIG. 10. Effect of [NaCl] on DTAC proton relaxation rates. [DTAC] = 0.1022 *M*. Slopes are (1) bulk methylene, 0.155; (2) *N*-methyl, 0.164; (3) terminal methyl, 0.113 s^{-1} M^{-1}.

different DTAC concentrations are shown in Figs. 13 and 14. The pH of the solutions used in the runs plotted in Fig. 13 was 8.5; in Fig. 14 the pH was 5.3. There is a marked increase in relaxation rates at the higher pH; presumably at the higher pH there are more negative sites on the floc at which the cationic DTAC can be adsorbed. At pH 5.3 the relaxation rates of the bulk methylene and *N*-methyl protons indicate only the effects of micelle formation. At pH 8.5 the relaxation rates show a sharp upturn at low surfactant concentrations, probably caused by the fact that a large fraction of the surfactant ions is adsorbed on the floc under these conditions. As one would expect, the effect is larger for the *N*-methyl protons than for the bulk methylene protons. The increase in relaxation rate of the terminal methyl protons seen in Fig. 14 suggests that at pH 5.3 the surfactant ions are adsorbed at the terminal methyl group rather than at the $N(CH_3)_3^+$ group. We note, however, that the terminal methyl peaks are quite weak at low surfactant concentrations, and therefore the determination of the terminal methyl relaxation times is not very accurate at low surfactant concentrations. The problem was even more acute at pH 8.5, which is why the relaxation rates of the terminal methyl protons are not shown in Fig. 13.

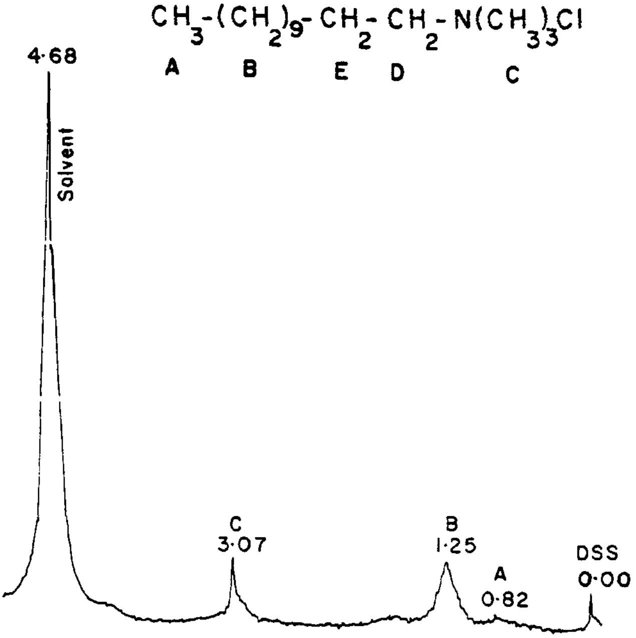

FIG. 11. Proton NMR spectrum of 0.0136 *M* DTAC in the presence of FeS–Al(OD)$_3$ floc. Instrument conditions as in Fig. 1.

Experiments with DTAC and Al(OD)$_3$ only (no FeS) at pD 5.8 yielded relaxation times virutally identical with those obtained in the absence of any floc, although the peaks were slightly broadened. Since alumina is positively charged at pH's below about 9 (*22*), it is unlikely that there would be adsorption of a cationic surfactant like DTAC on this floc.

A few measurements were made on solutions of dodecylammonium chloride, $CH_3(CH_2)_{11}ND_3^+Cl^-$ (DAC) in D_2O solution. The cmc of DAC at 25°C is given by Mukerjee and Mysels (*20*) as 14.6 m*M*. Two sets of runs were made. For those in Fig. 15, dodecylamine was reacted with HCl and the dodecylammonium chloride formed was then recovered by crystallization. This material was then used to make up the solutions, which were adjusted to pH 5.0. For the runs in Fig. 16, a standard solution of $CH_3(CH_2)_{11}ND_3^+Cl^-$ was made by reacting the amine with DCl in D_2O; this solution was used without further purification to make up the samples for the NMR measurements. The results show the expected increase in relaxation rate with increasing extent of micellization. We

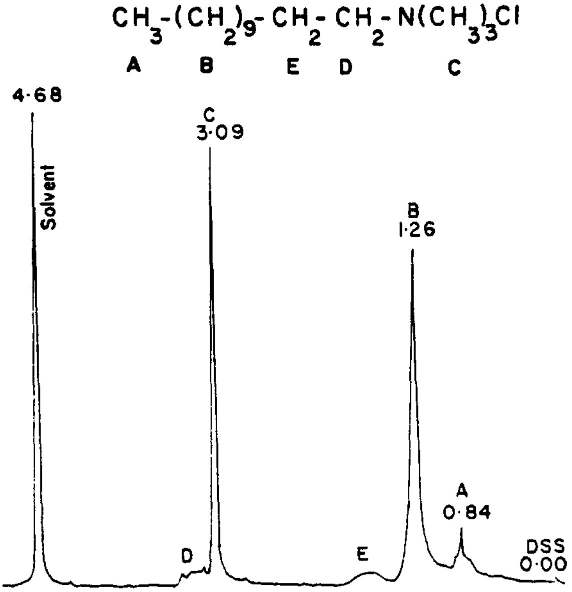

Fig. 12. Proton NMR spectrum of 0.1046 *M* DTAC in the presence of FeS–Al(OD)$_3$ floc. Instrument conditions as in Fig. 1.

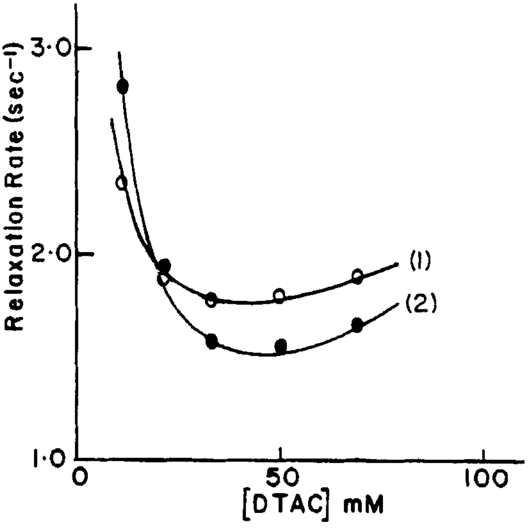

Fig. 13. DTAC proton relaxation rates versus DTAC concentration (m*M*) in the presence of FeS–Al(OD)$_3$ floc. (1) Bulk methylene; (2) *N*-methyl protons. The pH of these samples was 8.5.

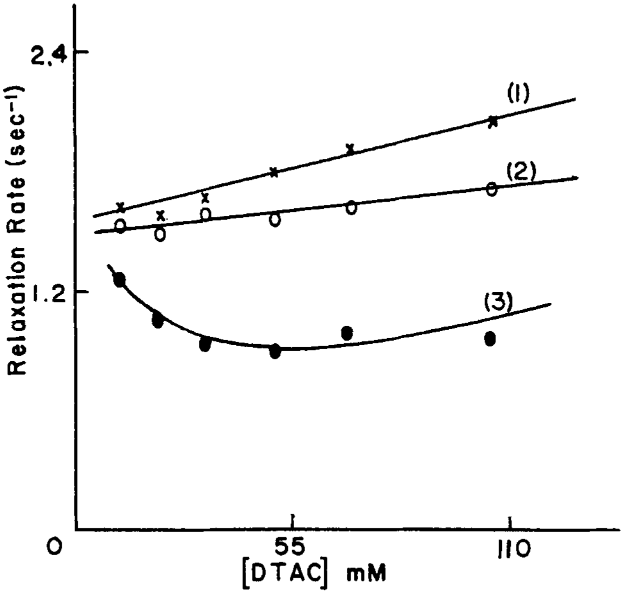

FIG. 14. DTAC proton relaxation rates versus DTAC concentration (m*M*) in the presence of FeS-Al(OD)$_3$ floc. (1) Bulk methylene; (2) *N*-methyl; (3) terminal methyl protons. The pH of these samples was 5.3.

speculate that the slight differences in the slopes in the two figures may be due to the difference in pH; this point requires further investigation.

THEORY

The T_1 measurements described above indicate that the protons in surfactant hydrocarbon chains in surfactant solutions above the cmc are increasingly constrained as the ionic strength of the solution increases. As mentioned above, it is known that the aggregation numbers for micelles of ionic surfactants increase with increasing ionic strength, and that the radius of a sperhical micelle is approximately equal to the length of the surfactant ion in its extended zigzag conformation. In this section we first present a rather simple theoretical model for the effect of ionic strength on micelle aggregation number; then we turn to a somewhat more elaborate treatment based on a nonlinear Poisson-Boltzmann equation which includes the effect of ionic size.

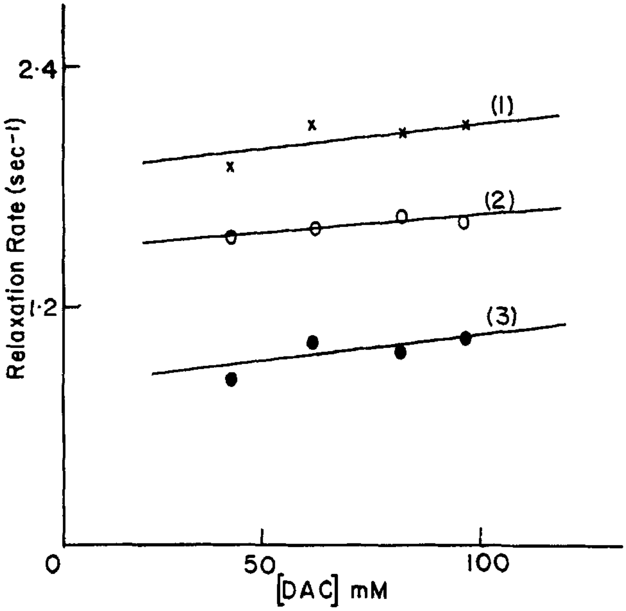

FIG. 15. DAC relaxation rates versus DAC concentration (m*M*). Slopes of the lines are as follows: (1) bulk methylene, 1.74 ± 0.96; (2) α-methylene, 2.98 ± 1.85; (3) terminal methyl, 3.1 ± 1.8 s^{-1} M^{-1}. Samples prepared from crystallized dodecylammonium chloride. pH = 5.0.

Simple Theory

Consider a system of N surfactant ions in solution; we form micelles of radius r_l containing n surfactant ions per micelle. We wish to choose n such that the free energy of micelle formation is minimized. The free energy is assumed to consist of an electrical component plus a surface tension component. The electrical component is calculated as follows.

According to the Debye-Hückel theory, the electric potential in the vicinity of a spherical micelle is given by

$$\psi(r) = \frac{A \exp(-\kappa r)}{r} \tag{2}$$

where

$$\kappa = \left(\frac{8\pi c_\infty z^2 e^2}{DkT}\right)^{1/2} \tag{3}$$

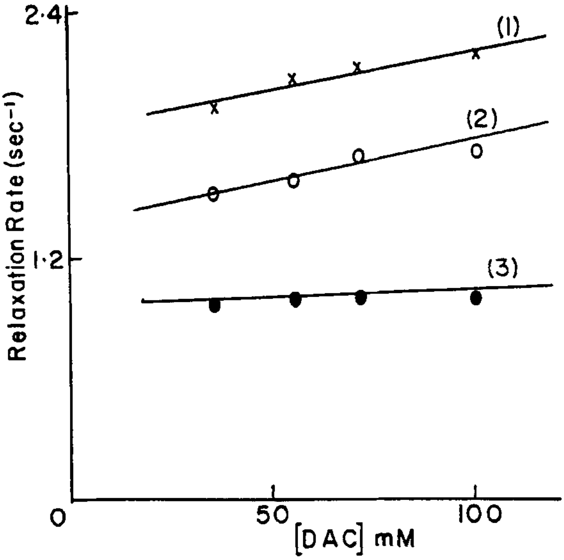

FIG. 16. DAC relaxation rates versus DAC concentration (m*M*). Slopes of the lines are: (1) bulk methylene, 4.0 ± 1.0; (2) α-methylene, 3.3 ± 0.8; (3) terminal methyl, 0.47 ± 0.17 s^{-1} M^{-1}. Samples prepared from a stock solution made by neutralizing dodecylamine with DCl solution.

and r = distance from the center of the micelle
c_∞ = salt concentration, ions/cm^3
z = ionic charge
e = magnitude of electronic charge
D = dielectric constant
k = Boltzmann's constant
T = temperature, °K
κ = Debye length, mean thickness of the ionic atmosphere

The electrical neutrality requirement gives

$$\left.\frac{\partial \psi}{\partial r}\right|_{r=r_1} = -\frac{4\pi\sigma}{D} \tag{4}$$

where σ is the surface charge density of the micelle, which we take as given by

$$\sigma = \frac{ne}{4\pi r_1^2} \tag{5}$$

$$\left.\frac{\partial\psi}{\partial r}\right|_{r=r_1} = -\frac{ne}{Dr_1^2} \tag{6}$$

This result can then be used to calculate the unknown constant in Eq. (2); the result is

$$\psi(r) = \frac{ne\exp(\kappa r_1)}{D(1+\kappa r_1)}\frac{\exp(-\kappa r)}{r} \tag{7}$$

which gives a micelle surface potential of

$$\psi(r)|_{r=r_1} = \frac{ne}{Dr_1(1+\kappa r_1)} \tag{8}$$

Next we calculate the electrical free energy of charging the surfactant ions by means of a Guntelberg charging process identical to that used in the Debye-Hückel theory. This gives

$$\Delta G_{\text{elec}} = \int_0^1 \psi(r_1,\lambda)Ned\lambda \tag{9}$$

where

$$\psi(r_1,\lambda) = \frac{ne\lambda}{Dr_1(1+\kappa r_1)} \tag{10}$$

The result is

$$\Delta G_{\text{elec}} = \frac{Nne^2}{2Dr_1(1+\kappa r_1)} \tag{11}$$

The nonelectrical free energy of a single micelle we take as

$$\Delta G^1_{\text{nonelec}} = \varepsilon_s \cdot 4\pi r_1^2 \tag{12}$$

The number of micelles is given by N/n, so the nonelectrical energy of the system is given by

$$\Delta G_{\text{nonelec}} = \frac{N}{n}\Delta G^1_{\text{nonelec}} = \frac{N}{n}\varepsilon_s \cdot 4\pi r_1^2 \tag{13}$$

The total free energy of micelle formation is just the sum of Eqs. (11) and (13),

$$\Delta G_{\text{total}}(n) = N\left[\frac{e^2 n}{2Dr_1(1 + \kappa r_1)} + \frac{\varepsilon_s \cdot 4\pi r_1^2}{n}\right] \tag{14}$$

This must be minimized with respect to n, so

$$\frac{\partial \Delta G_{\text{total}}}{\partial n} = 0 = N\left[\frac{e^2}{2Dr_1(1 + \kappa r_1)} - \frac{\varepsilon_s \cdot 4\pi r_1^2}{n^2}\right] \tag{15}$$

Solving Eq. (15) for n then gives

$$n = \left[\frac{8\pi\varepsilon_s D r_1^3(1 + \kappa r_1)}{e^2}\right]^{1/2} \tag{16}$$

where we recall that

$$\kappa = \left(\frac{8\pi c_\infty z^2 e^2}{DkT}\right)^{1/2} \tag{3}$$

It is evident from Eqs. (16) and (3) that the aggregation number n increases with increasing salt concentration c_∞, and that, for given c_∞, the aggregation number is larger for $z = 2$ than for $z = 1$. It should be noted that there is a maximum value for n, given approximately by

$$n_{\max} = \tfrac{4}{3}\pi r_1^3 N_0/\bar{V} \tag{17}$$

where N_0 = Avogadro's number
$\bar{V}$ = molar volume of the surfactant ion

Therefore one should regard aggregation numbers calculated from Eq. (16) as meaningful only if they are less than $n_{\max}$.

Representative plots of n versus $\log_{10} c_\infty$ for $z = 1$ and $z = 2$ are shown in Fig. 17. The results are in approximate agreement with the aggregation numbers given for dodecyltrimethylammonium bromide (50) and dodecyltrimethylammonium sulfate (65) at 23°C in Rosen's book (*23*). We note that as n increases at constant micelle radius, the surfactant hydrocarbon chains become more and more closely packed, thereby constraining the motions of the protons, in agreement with the results of our relaxation time measurements.

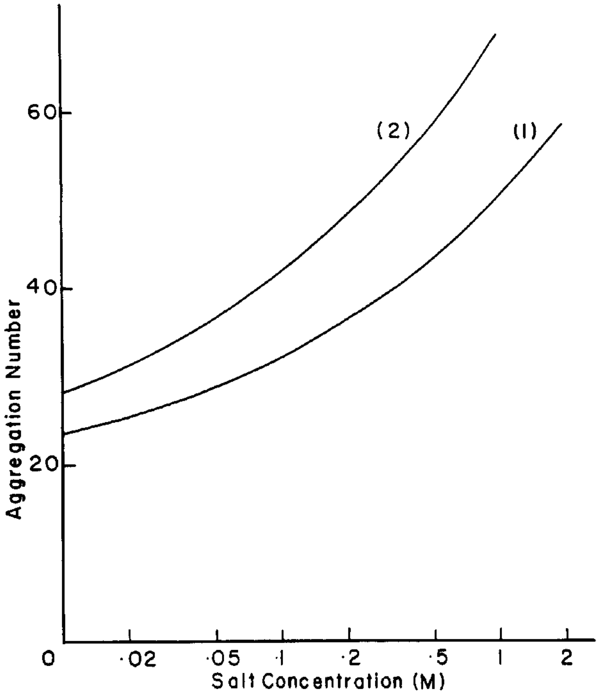

FIG. 17. Plots of DTAC aggregation number versus inert salt concentration, simple theory. $\bar{V} = 291$ cm^3; $\varepsilon_s = 5.0$ erg/cm^2; $r_1 = 20$ Å; $D = 78$; $T = 298$ °K; $z = 1$ (bottom), 2 (top). $n_{\max} = 69$ for these micelles.

Nonideal Theory

The model for calculating micelle aggregation numbers described above suffers from at least two deficiencies. The linearized Poisson-Boltzmann equation used to obtain Eq. (2) replaces exponential Boltzmann factors with linear approximations which are quite poor. Also, that Poisson-Boltzmann equation does not take into account the finite sizes of the ions in the ionic atmospheres of the micelles. In this section we develop a model which takes these two points into account. We must pay a price, however, in that it is necessary to use planar symmetry instead of the correct spherical symmetry.

The Poisson-Boltzmann equation is

$$\nabla^2\psi = -4\pi\rho/D \tag{18}$$

where ρ is the charge density at the point r in the solution. We develop this equation by the method of Macdonald and Brachman (*24*), used by us earlier (*25*, *26*) in connection with adsorbing colloid flotation theory. We briefly summarize the development.

The charge density is given by

$$\rho(r) = ez[c^+(r) - c^-(r)] \tag{19}$$

where z = magnitude of ionic charge, assumed the same for anion and cation

$c^+(r)$ = concentration of cations at r, ions/cm^3

$c^-(r)$ = concentration of anions at r

To take the finite volumes of the ions into account, we assume that the electrochemical potentials of the anion and cation are given by

$$\mu^+(r) = \mu_0^+ + kT\log_e\left[c^+\frac{c_{\max}}{c_{\max} - c^+ - c^-}\right] + ze\psi \tag{20}$$

$$\mu^-(r) = \mu_0^- + kT\log_e\left[c^-\frac{c_{\max}}{c_{\max} - c^+ - c^-}\right] - ze\psi \tag{21}$$

We have assumed that the effective ionic volumes of the anion and cation are sufficiently similar that they may be approximated as equal. The term $c_{\max}/(c_{\max} - c^+ - c^-)$ is an activity coefficient designed to take into account the finite sizes of the ions; $c_{\max}$ represents a maximum possible concentration of ions, a limit set by their finite sizes.

Equilibrium requires that the electrochemical potentials be independent of position; this gives

$$kT \log_e \frac{c_\infty c_{\max}}{c_{\max} - 2c_\infty} = kT \log_e \frac{c^+ c_{\max}}{c_{\max} - c^+ - c^-} + ze\psi \tag{22}$$

and

$$kT \log_e \frac{c_\infty c_{\max}}{c_{\max} - 2c_\infty} = kT \log_e \frac{c^- c_{\max}}{c_{\max} - c^+ - c^-} - ze\psi \tag{23}$$

One then solves Eqs. (22) and (23) simultaneously for c^+ and c^-, substitutes these results into Eq. (19) to obtain the charge density, and substitutes this into Eq. (18) to obtain the following Poisson-Boltzmann equation:

$$\nabla^2\psi = \frac{A \sinh(ze\psi/kT)}{1 + B \cosh(ze\psi/kT)} \tag{24}$$

$$A = \frac{8\pi zec_{\max}c_\infty}{D(c_{\max} - 2c_\infty)} \tag{25}$$

$$B = \frac{2c_\infty}{c_{\max} - 2c_\infty} \tag{26}$$

The requirement of electrical neutrality yields Eq. (4) as a boundary condition for Eq. (24), and a second boundary condition is

$$\lim_{r\to\infty} \psi(r) = \lim_{r\to\infty} |\nabla\psi| = 0 \tag{27}$$

One would like to integrate Eq. (24) in spherical coordinates at least to obtain a first integral, from which one would get an equation relating micelle surface charge density and micelle surface potential. This is not possible to do in closed form. In view of the fact that one must carry out an integration of the surface potential as a function of the Guntelberg charging parameter λ (see Eq. 9), lack of a closed form solution for the surface potential in spherical coordinates is especially unfortunate. We therefore approximate by using the solution to Eq. (24) which is appropriate for a plane surface rather than a sphere. The Poisson-Boltzmann equation then becomes

$$\frac{d^2\psi}{dx^2} = \frac{A \sinh(ze\psi/kT)}{1 + B \cosh(ze\psi/kT)} \tag{28}$$

A first integral for Eq. (28) is readily obtained by Newton's method. The electrical neutrality requirement is

$$\left.\frac{d\psi}{d\psi}\right|_{x=r_1} = -\frac{4\pi\sigma}{D} = -\frac{ne}{Dr_1^2} \tag{29}$$

where n = number of surfactant ions in a micelle
r_1 = radius of micelle

The desired first integral to Eq. (28) which satisfies the boundary conditions (Eqs. 27 and 29) is

$$\left(\frac{4\pi\sigma}{D}\right) = \frac{2AkT}{zeB} \log_e \frac{1 + B \cosh(ze\psi_0/kT)}{1 + B} \tag{30}$$

where ψ_0 is the surface potential of the micelle. Solving this for ψ_0 and substituting the expressions for A, B and σ then yields

$$\psi_0(r_1,\lambda) = \frac{kT}{ze} \operatorname{argcosh} \left\{\frac{c_{\max}}{2c_\infty}\left(\exp\left[\frac{(ne/r_1^2)^2\lambda^2}{8\pi DkTc_{\max}}\right] - 1\right) + 1\right\} \tag{31}$$

where we have included the Guntelberg charging parameter in the expression.

The electrical free energy of N surfactant ions forming micelles of radius r_1 and containing n surfactant ions per micelle is again given by Eq. (9), with ψ given by Eq. (31). We keep Eq. (12) for the nonelectrical free energy of a single micelle, so the expression for the total free energy of the system of N surfactant ions is given by

$$\Delta G_{\text{total}}(n_1 r_1) = N\left\{\frac{kT}{z}\int_0^1 \operatorname{argcosh}\left\{\frac{c_{\max}}{2c_\infty}\left(\exp\left[\frac{(ne/r_1^2)^2\lambda^2}{8\pi DkTc_{\max}}\right] - 1\right) + 1\right\}\right.$$

$$\left. \times\, d\lambda + \frac{4\pi\varepsilon_s r_1^2}{n}\right\} \tag{32}$$

We note that both the simple theory discussed in the previous section and this theory calculate ΔG_{elec} for a process other than taking the charge off of the single surfactant ions in the solution and then recharging these ions after they have been formed into micelles. These ΔG_{elec} values are therefore not suitable for use in calculating equilibrium constants for micelle formation, cmc's, etc., since they are not referenced to non-micellized surfactant ions in electrolyte solution. This, however, causes no difficulty in determining the value of n which makes the free energy a minimum.

Evidently there is the same upper limit for n, $n_{\max}$, which was determined for the simple theory; see Eq. (17).

Parameters for use in these theoretical models were obtained as follows. The molar volume of the dodecyltrimethylammonium ion was estimated in two ways. First, the volume of the alkyl chain was estimated by extrapolating molar volumes of *n*-alkyl amines; this yielded a molar volume for the chain of 17.13 cm^3 times the number of carbons in the chain. The volume of an *N*-methyl group less the volume of a hydrogen was determined by comparing the molar volumes of *n*-propylamine and *n*-butylamine with the molar volumes of the *N*-methyl-substituted compounds; this gives a volume of 19.38 $\mathrm{cm}^3/\mathrm{mol}$. The molar volume of dodecyltrimethylammonium ion was then calculated as the molar volume of *n*-octylamine plus 4 × molar volume of CH_2 + 3 × molar volume of an *N*-methyl less the molar volume of H. This yields a value of 292.99 $\mathrm{cm}^3/\mathrm{mol}$. Estimation by using the molar volume of lauryl amine plus 3 × molar volume of an *N*-methyl less that of H yielded a value of 289.39 $\mathrm{cm}^3/\mathrm{mol}$. These were averaged to give the molar volume actually used, 291 $\mathrm{cm}^3/\mathrm{mol}$.

The radius of a micelle was assumed to be slightly larger than the extended length of a 12-carbon alkyl chain; a value of 20 Å was used. The crystal radii of chloride and sulfate were taken as 1.81 and 3.05 Å, respectively, and the dielectric constant of water was taken to be 78. The temperature was assumed to be 298 K, and the nonelectrical surface energy of the micelle was selected to be 5 $\mathrm{erg/cm}^2$ to fit the data. Given the micelle radius and the molar volume of the surfactant, the maximum number of surfactant ions which can be crowded into a micelle is 69. The ionic radii for chloride and sulfate lead to $c_{\max}$ values of 33.4 and 7.0 *M*, respectively.

Representative plots of aggregation number n versus $\log_{10} c_\infty$ for $z = 1$ and $z = 2$ are given in Fig. 18. The results appear to be in fairly good agreement with experimental data on aggregation numbers, and are consistent with our T_1 findings. We note that there is better agreement than one might expect between these results and the results of the simple theory presented earlier in this paper (see Fig. 17). Also, we again point out that this more elaborate model is flawed by the use of planar, rather than spherical, geometry in the Poisson-Boltzmann equation.

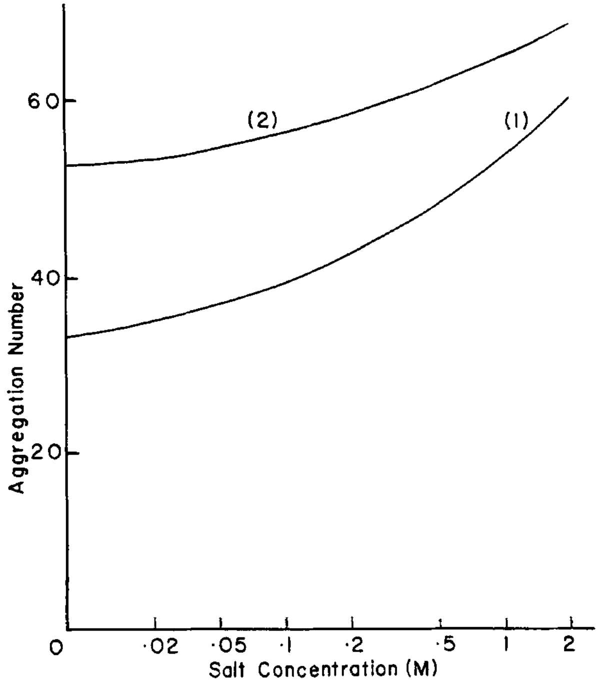

FIG. 18. Plots of DTAC aggregation number versus inert salt concentration, nonideal theory. For curve (1), $z = 1$, $c_{\max} = 33.4\ M$; for curve (2), $z = 2$, $c_{\max} = 7.0\ M$. Other parameters as in Fig. 17.

Acknowledgment

This work was supported by a grant from the National Science Foundation.

REFERENCES

1. B. Lindman and P. Stilbs, *Proc. Int. Sch. Phys.; Enrico Fermi, 90,* 94-121 (1985).
2. O. Soederman, *Nucl. Magn. Reson., 14,* 350-383 (1985).
3. C. Taupin, *Colloides Interfaces, Ec. Ete.,* pp. 215-242 (1983; published 1984).
4. P. Nilsson, H. Wennerstrom, and B. Lindman, *J. Phys. Chem., 87,* 1377 (1983).
5. P. Nilsson and B. Lindman, *Ibid., 88,* 5391 (1984).
6. J. C. Erikson and G. Gilberg, *Acta Chem. Scand., 20,* 2019 (1966).
7. P. Stilbs, *Chem. Scr., 19,* 93 (1982).
8. P. G. Nilsson, H. Wennerstrom, and B. Lindmann, *Ibid., 25,* 67 (1985).
9. B. Persson, T. Drakenberg, and B. Lindman, *J. Phys. Chem., 83,* 3011 (1979).
10. T. Yoshida, K. Taga, H. Okabayshi, K. Matsushita, H. Kamaya, and I. Ueda, *J. Colloid Interface Sci., 109,* 336 (1986).
11. G. J. T. Tiddy, K. Rendall, and M. A. Trevethan, *Comun. Jorn. Com., Esp. Deterg., 15,* 51-62 (1984).
12. M. M. Chobanau, V. M. Ropot, and S. F. Manole, *Izv. Akad. Nauk Mold. SSR, Ser. Biol. Khim. Nauk, 3,* 72-74 (1984).
13. E. E. Zeev and L. M. Khalilov, *Kolloidn. Zh., 46,* 427-432 (1984).
14. N. N. Kalibabchuk and L. K. D'yachek, *Ibid., 42,* 629-633 (1980).
15. K. Kalyanasundaram, M. Graetzel, and J. K. Thomas, *J. Am. Chem. Soc., 97,* 3915-3922 (1975).
16. R. D. Vold and M. J. Vold, *Colloid and Interface Chemistry,* Addison-Wesley, Reading, Massachusetts, 1983, p. 597.
17. H. F. Huisman, *Proc. K. Ned. Akad. Wet., Ser. B, 67,* 368 (1964).
18. W. Abraham, T. M. Harris, and D. J. Wilson, *Sep. Sci. Technol., 19,* 389 (1984).
19. M. Sarker, M. Bettler, and D. J. Wilson, *Ibid., 22,* 47 (1987).
20. P. Mukerjee and K. J. Mysels, *Critical Micelle Concentrations of Aqueous Surfactant Systems,* National Bureau of Standards, U.S. Department of Commerce, Washington, D.C., 1971.
21. Asahi Research Center, *Handbook of Proton NMR Spectra and Data,* Vol. 5, Academic, New York, 1985, p. 148, spectrum 3491.
22. D. W. Fuerstenau, *Chem. Biosurfaces, 1,* 143 (1971).
23. M. J. Rosen, *Surfactants and Interfacial Phenomena,* Wiley, New York, 1978, p. 90.
24. J. R. Macdonald and M. K. Brachman, *J. Chem. Phys., 22,* 1314 (1954).
25. D. J. Wilson, *Sep. Sci., 11,* 391 (1976).
26. J. E. Kiefer and D. J. Wilson, *Sep. Sci. Technol., 15,* 57 (1980).

Received by editor September 17, 1987